The 2009 IEEE/RSJ International Conference on
Intelligent Robots and Systems
October 11-15, 2009 St. Louis, USA

A Fluoroscopic-Based Navigation System for ACL Reconstruction Assisted by Robot

Yan Hu, Lei Hu, Tianmiao Wang, Jun Wei, Lei Sun, Wenyong Liu, Li Wen, *Member, IEEE*

Abstract—**Entry position of the graft is very important in anterior cruciate ligament (ACL) reconstruction. However the determination of entry position is very difficult to the surgeon. In this paper, a navigation and evaluation system assisted by the 6-DOFS robot is implemented for the simulation evaluation and planning insertion points based on quadrant method for the femur and Stäublis method for the tibia on the lateral X-ray image of knee joint. Meanwhile, the implementation of the key technologies such as image correction, image registration, C-arm calibration, video tracking, bone surface reconstruction, image fusion, 6-DOFS robot, and virtual simulation are introduced. Finally, Experiments about the tunnel planning method and real time tracking of surgical apparatus are implemented on 8 bone of plastic models (Sawbone, Swiss) and 10 bones of the goat. In the experiment, the tibia rotates around the femur under the surgeon's implementation to evaluate the planning result with the virtual simulation and evaluation module. The positioning error is 1.59mm from analysis on 30 space targets. The virtual reconstruction ACL is satisfied with two important criteria of the best isometry and collision detection between graft and intercondylar surface of femur. The results are well accepted in operations. In order to satisfying with the request of exact operation in ACL reconstruction, we have developed 6-DOFS passive robot to assist the surgeons entry positioning and drilling of implant tunnels, implementing exact operation in knee joint.**

I. Introduction

THE rupture of Anterior Cruciate Ligament (ACL) is one of the most familiar sport injury and very common among young athletes. The injured ACL is difficult to rehabilitate and causes knee instability, the damage of meniscus and cartilage, and function degeneration of knee if not healed as early as possible [1]. The position of graft's the insertion points are very difficult to confirm, so the function failure-rate of ACL could reach up to 8%, even 25% in the traditional ACL reconstruction operation [2-4]. The instability of the knee joint can't be controlled easily because the anisometric ACL implantation may be elongated. Radiological studies indicate that approximately 10% to 40% of drill holes in ACL reconstructions have been incorrectly placed. And error analysis studies on failed ACL reconstructions show that incorrectly placed drill holes cause graft failure at a rate of 73.5% [5]. So, one of the main problems during reconstruction is to find the optimal attachment positions for the graft [6].

Computer aided orthopaedic surgery (CAOS) provides new means for this problem as it can improve the position precision [7]. In the past years, many studies have been done on the ACL reconstruction navigation operations in the world, for example, KneeNav ACL system developed by Medical Center of University of Pittsburgh incorporating associating with Medical Robot and Computer Aided Surgery Center (MRCAS) of University of Carnegie Mellon is an ACL navigation system based on the planning on the intra-operation CT image and tracking the patient and probe through the optical tracker in real time [8]. The VectorVision navigation system, which developed by BrainLab of Germany realized Image Guided Surgery (IGS) based on fluoroscopic image and photoelectric navigation [9], provides real-time navigation to tracking the insert position of tunnel through photoelectric navigation equipment. They implement operation planning with quadrant of femur and Stäublis of tibia, and gather the vision effect of operation through displaying instrument on the fluoroscopic image. The Orthopilot navigation system of Tuttlingen Inc. of Germany validates isometry characteristic between femur and tibia and detects collision between graft and inter-condyle [10]. Mamoru [11] and Jaramaz [12] carried through ACL reconstruction navigation with X-ray and MRI respectively.

Many study results and some mature products which are very expensive yet have been gotten and developed by some international study institute. The arthroscopic operation will not be popular because of its difficulty for surgeons. Moreover, the precision of the graft can not been guaranteed and the stability is not well because the manipulation is mostly dependent on the surgeon's experience.

Manuscript received February 15, 2009. (Write the date on which you submitted your paper for review.) This work was supported in part by the National High Technology Research and Development Programme of China (No.2004AA421022), National Science Fund for Distinguished Young Scholars of P. R. China (No.60525314) and National Science & Technology Pillar Program in the Eleventh Five-year Plan (No.2006BAI03A16)

Y. Hu was with the Robotics Institute, Beijing University of Aeronautics and Astronautics, Beijing 100191 China. He is now with Control Science and Engineering Department, University of Jinan, Jinan, Shandong 250022, China. (corresponding author to provide phone: 86-010-82338272; fax: 86-010-82338271; e-mail: buaarobot@126.com).

L. Hu is with Robotics Institute, Beijing University of Aeronautics and Astronautics, Beijing 100191, China. (e-mail: hulei9971@126.com).

T. M. Wang is with the Robotics Institute, Beijing University of Aeronautics and Astronautics, Beijing 100191, China. (e-mail: wtm_itm@263.net).

J. Wei is with Control Science and Engineering Department, University of Jinan, Jinan, Shandong 250022, China. (e-mail: cse_wj@ujn.edu.cn)

L. Sun is with the Beijng Institue of Traumatology and Orthopedics, Jishuitan Hospital, Beijing 100035, China (e-mail: dr_sunlei@263.net).

Aiming at the problems above, this work plans the graft's insertion point on two corrected X-ray images based on the femoral quadrant and tibial Stäublis accepted in medicine field widely. Moreover, this system utilizes precise position of computer-aided navigation and the video tracking enhancing the vision effect. And in the real-time tracking of the video, the operation instruments can be projected on the X-ray images. Then 3D information of insertion points can be planned as well as the direction of implantation tunnels. Finally, whether the graft satisfies the criterion of isometry and collides with the intercondyle through the reconstructed ACL is simulated. So it can avoid iterative harm to the patient and improve the veracity and efficiency because it can help the surgeon adjust the operation in time.

II. Material and Method

The system includes several modules such as the image acquisition, the image dewarping, the C-arm calibration, MicroTracker2.7 camera based video, NDI camera based photoelectric, passive robot of 6-DOFS, operation controlling platform, intraoperative bone surface reconstruction and virtual simulation, as shown in Fig.1.

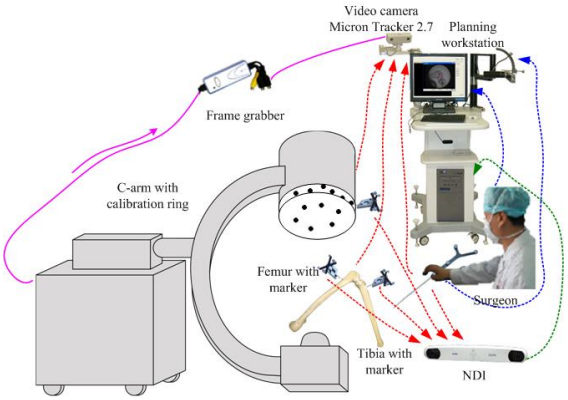

Fig 1. Diagram of system configuration

The system captures two lateral X-ray images for the femur and tibia installed with DRB using C-arm, corrects them to provide fluoroscopic in case of distortion. And the registration matrix of operation instrument on fluoroscopic can be acquired through the C-arm's registration by using two-layer correction board installed on the C-arm. Then the operation can be planned on X-ray images based on femoral quadrant and tibia Stäublis method, and the implantation points can be explored by the operation instrument with DRB. Then, the surgeon can collect the surfaces' characteristic through the operation instruments' gliding on the femoral intercondyle and tibia platform to drill the tunnel assisted by the 6 DOFS robot. Finally, virtual ACL can be reconstructed and the kinematics of knee joint can be simulated to evaluate the isometric characteristic and whether colliding with femoral intercondyle.

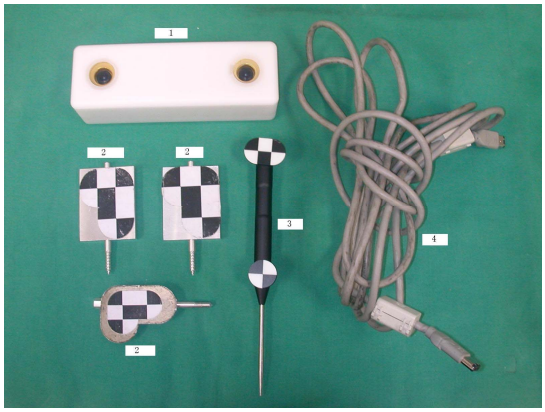

Fig. 2. Micron Tracker and probe with Marker. 1.Camera with two sensors 2.Marker 3.Probe 4.1394 cable

III. Key Algorithm and Technology's Implement

A. Video Tracking

As shown in Fig.2, the optical navigation equipment MicronTracker, produced by Claron Technology Company in Canada, is a completely passive camera with two sensors, which can track the object's position and orientation in the field of measurement (FOM). MTC supports over 200 functions, enabling the application to tightly control and modify many aspects of MicronTracker's hardware and software operations. Combined with the characteristic of ACL operation, feasible procedure according to the video monitor is developed by this function library, and it includes:

(1) Call function Cameras_AttachAvailableCameras() to establish the communication link with all the cameras physically connected to the computer, and load the proper calibration file for each of the cameras;

(2) Call function Markers_LoadTemplates() to load all the marker templates files;

(3) Call function Cameras_GrabFrame() to obtain the recent frame images from the camera(s);

(4) Call function Markers_ProcessFrame() to update the collection of Identified markers;

(5) Call function Markers_IdentifiedMarkersGet() to collect of the handles of the identified markers;

(6) Call function Marker_Marker2CameraXfGet() to

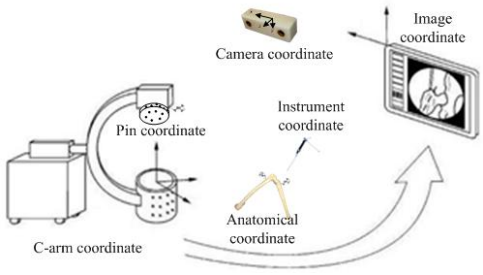

Fig. 3. The coordinate transformation

TABLE I
SURGICAL OBJECTS' COORDINATES IN THE OPERATION ENVIRONMENT

serial number	*Coordinate*	Abbreviated Name	*Description*
1	Tool	T	Marker coordinate on the operation instrument
2	Micron Tracker	M	Micron Tracker coordinate
3	Anatomical	A	Marker coordinate on the knee joint
4	C-arm	C	Marker coordinate on the calibration board
5	Pinhole	S	Coordinate of steel ball installed on the calibration board
6	Image	I	X-ray image coordinate

obtain the location and orientation of identified markers;

B. Coordinate Transformation and C-arm Registration

By marking the surgical object and surgical instruments, different coordinate systems are established. The space relation is shown in Fig.3 and the coordinate definition of every object in the operation is shown in Table 1.

Suppose ${}^{M}_{T}T$, ${}^{C}_{M}T$ and ${}^{A}_{M}T$ as the transformation matrix from instrument coordinate to camera coordinate, camera coordinate to C-arm coordinate, and camera coordinate to anatomical module coordinate. So the transformation matrix from the instrument coordinate to the pinhole coordinate could be acquired from the Micron Tracker as $V_S = {}^{S}_{C}T\,{}^{C}_{M}T\,{}^{M}_{B}T\,{}^{B}_{M}T\,{}^{M}_{T}T V_T$.

C. Images Correction Algorithm

Distortion of fluoroscopic images acquired by c-arm often influences the navigation precision of the operation. But there is a most optimized mapping coefficient matrix between the distorted and ideal image because they are both composed of several discrete pixel points and they are one-to-one corresponding. This work estimates the project distortion of c-arm through polynomial fitting to avoid complex geometry modeling and distorted images correction step-by-step. The binary Nst-order polynomial can be represented as followed.

$$p = [a_0 \cdots a_j \cdots a_M] \times S \tag{1}$$

The fitting result, the coefficient of polynomial, and the vector composed of scattered points are defined as p, aj, and S respectively. The formulation of S is a vector [1 x y … x_N … x_N-k … y_N]^T and x and y represent the component coordinate of the scattered points. So the mapping between ideal image and distorted image can be realized from formula (1).

$$\begin{bmatrix} p_i \\ q_i \end{bmatrix} = \begin{bmatrix} a_0 & \cdots & a_j & \cdots & a_M \\ b_0 & \cdots & b_j & \cdots & b_M \end{bmatrix} \times S_i \tag{2}$$

Where a_j and b_j are correction coefficients, a_0 and b_0 present the shift in X and Y direction respectively, a_1, b_1, a_2 and b_2 represent the rotation of pixels points. As j > 2, a_j and b_j have no specific physical mean. The formula $M = \sum_{i=0}^{N} (i+1)$ represents the number of correction coefficient in X or Y direction. N is order of the polynomial and N≥3.

$$S = [1 \quad x_i \quad y_i \quad \cdots \quad x_i^N \quad \cdots \quad x_i^{N-k} \quad y_i^k \quad \cdots \quad y_i^N]^T \tag{3}$$

(x_i, y_i) and (p_i, q_i) is the coordinate of points on the ideal and distorted image respectively. So the correction coefficients will be increased as orders of polynomial increased. The formula (3) can be deduced into 2K formulas.

$$\begin{bmatrix} p_1 \\ q_1 \\ \vdots \\ p_K \\ q_K \end{bmatrix} = \begin{bmatrix} a_0 & \cdots & a_j & \cdots & a_M \\ b_0 & \cdots & b_j & \cdots & b_M \\ & & \vdots & & \\ a_0 & \cdots & a_j & \cdots & a_M \\ b_0 & \cdots & b_j & \cdots & b_M \end{bmatrix} \begin{bmatrix} S_1 \\ S_1 \\ \vdots \\ S_K \\ S_K \end{bmatrix}^T \tag{4}$$

The formula (4) is an over-determined linear equation whose least-squares solutions are the most optimized global correction coefficients. The mapping between distorted and ideal images can be realized with these coefficients.

The correction board is made based on the requirement of algorithm as shown in Fig.4. The correction board is a

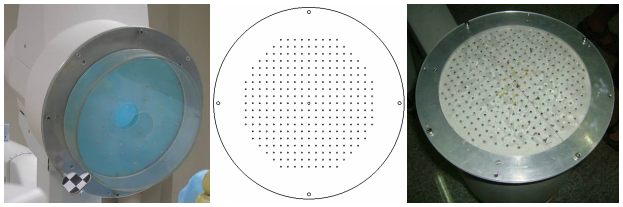

(a) (b) (c)

Fig. 4. The registration and correction module. (a) Two-layer Correction board (b) The principle of correction board (c) The correction board fixed on C-arm

PMMA disc whose diameter is 326mm and thickness 3mm. And there are 196 steel balls with 3mm diameter distributing equably on the correction board as the marker. The distance between each two is 12mm and another steel ball whose diameter is 4mm is located at the center. As shown in Fig.4 (b), the correction board is equipped on the connect board through bolt directly.

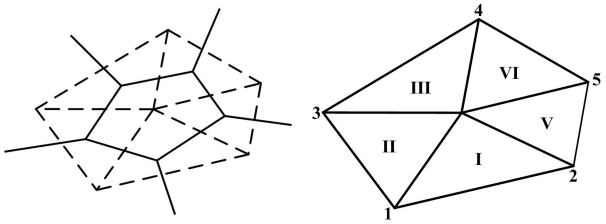

(a) (b)

Fig. 5. Delaunay Triangle (a) Dirichlet Polygon (b) Delaunay Triangle

D. Intra-operation Bone Reconstruction Algorithm

The intra-operation reconstruction of knee joint surfaces uses Delaunay triangulation algorithm, which originates from Dirichlet polygon. If we draw an adjacent area near every net point, the distance between any point in this area and the net point is less than that between this point and other net points. The adjacent area is called Dirichlet Polygon (shown in Figure 5(a)). Then we connect points in every polygon with net points in the adjacent polygon. It can construct a triangle called Delaunay Triangle, which is shown in Fig.5 (b) [13].

Delaunay algorithm in this paper is computed by the mean of point by point insertion iteration, and the procedure is followed in detail:

(1) Judge the relation of new net points with the circumcircle of each triangular. If the point is inside of the circumcircle of triangular, the triangular has to rebuild;

(2) Collect the rebuilding triangular required, then delete the adjacent edge and construct a protrusive polygon;

(3) Find the exterior border of the polygon, and connect the adjacent edges into a loop with the adjacent relation of these edges;

(4) Take out the two adjacent net points on the loop, and constructs triangular combining with new net points. Then compute its circumcenter and reconstruct the information of adjacent triangular. Then save the net points of triangular and the information of adjacent triangular into the array which includes the triangular by Delaunay triangulation;

(5) Replace the new triangular data structure array above as the triangular data structure array requiring rebuilding, then get new structure array after reordering those triangular.

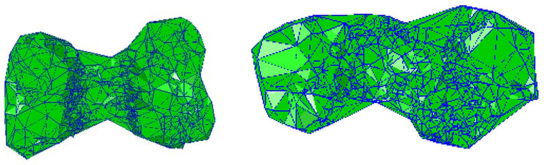

(a) (b)

Fig. 6. The reconstructed Knee Joint Surface. (a) Femur (b) Tibia

Although ACL reconstruction is performed on the femur/tibia with complex surface, Delaunay algorithm satisfies with the requirement of the authenticity, the complexity of local area and the real-time capability exactly. The surface reconstructed by Delaunay algorithm is shown in Fig.6.

E. Intra-operation Bone Reconstruction Algorithm

In order to satisfying with the request of exact operation in ACL reconstruction, we have developed 6-DOFS passive robot to assist the surgeons entry positioning and drilling of implant tunnels, implementing exact operation in knee joint. The operation security of assisted robot is improved because its mechanism adopts PRPRR configuration and its workspace and position adopts step control. As shown in Fig.7, passive robot and video camera are installed on the control platform.

The transform matrix is $T = A_1 \cdot A_2 \cdot A_3 \cdot A_4$. A_1, A_2, A_3, A_4 represent the coordinate transform matrix of 1, 2, 3, 4 joint, and d_1, d_2, d_3, d_4 represent the length of four arms respectively. 1 and 0 coordinate systems are rotation joints, and the arm's length is d_1. The transformation matrix is following.

$$A_1 = Rot(Z_0,\theta_1)Trans(0,d_1,0)$$

$$= \begin{bmatrix} \cos\theta_1 & -\sin\theta_1 & 0 & 0 \\ \sin\theta_1 & \cos\theta_1 & 0 & 0 \\ 0 & 0 & 1 & 0 \\ 0 & 0 & 0 & 1 \end{bmatrix} \begin{bmatrix} 1 & 0 & 0 & 0 \\ 0 & 1 & 0 & d_1 \\ 0 & 0 & 1 & 0 \\ 0 & 0 & 0 & 1 \end{bmatrix}$$

$$= \begin{bmatrix} \cos\theta_1 & -\sin\theta_1 & 0 & -d_1\sin\theta_1 \\ \sin\theta_1 & \cos\theta_1 & 0 & d_1\cos\theta_1 \\ 0 & 0 & 1 & 0 \\ 0 & 0 & 0 & 1 \end{bmatrix}$$

2 and 1 coordinate systems are rotation joints, and the arm's length is d_2. The transformation matrix is following.

$$A_2 = Rot(Z_1,\theta_2)Trans(0,d_2,0)Rot(Y_1,-90^\circ)$$

$$= \begin{bmatrix} \cos\theta_2 & -\sin\theta_2 & 0 & 0 \\ \sin\theta_2 & \cos\theta_2 & 0 & 0 \\ 0 & 0 & 1 & 0 \\ 0 & 0 & 0 & 1 \end{bmatrix} \begin{bmatrix} 1 & 0 & 0 & 0 \\ 0 & 1 & 0 & d_2 \\ 0 & 0 & 1 & 0 \\ 0 & 0 & 0 & 1 \end{bmatrix} \begin{bmatrix} 0 & 0 & -1 & 0 \\ 0 & 1 & 0 & 0 \\ 1 & 0 & 0 & 0 \\ 0 & 0 & 0 & 1 \end{bmatrix}$$

$$= \begin{bmatrix} 0 & -\sin\theta_2 & -\cos\theta_2 & -d_2\sin\theta_2 \\ 0 & \cos\theta_2 & -\sin\theta_2 & d_3\cos\theta_2 \\ 1 & 0 & 0 & 0 \\ 0 & 0 & 0 & 1 \end{bmatrix}$$

3 and 2 coordinate systems are rotation joints, and the arm's length is d_3. The transformation matrix is following.

$$A_3 = Rot(Z_2,\theta_3)Trans(0,d_3,0)$$

$$= \begin{bmatrix} \cos\theta_3 & -\sin\theta_3 & 0 & 0 \\ \sin\theta_3 & \cos\theta_3 & 0 & 0 \\ 0 & 0 & 1 & 0 \\ 0 & 0 & 0 & 1 \end{bmatrix} \begin{bmatrix} 1 & 0 & 0 & 0 \\ 0 & 1 & 0 & d_3 \\ 0 & 0 & 1 & 0 \\ 0 & 0 & 0 & 1 \end{bmatrix} = \begin{bmatrix} \cos\theta_3 & -\sin\theta_3 & 0 & -d_3\sin\theta_3 \\ \sin\theta_3 & \cos\theta_3 & 0 & d_3\cos\theta_3 \\ 0 & 0 & 1 & 0 \\ 0 & 0 & 0 & 1 \end{bmatrix}$$

4 and 3 coordinate systems are rotation joints, and the arm's length is d_4. The transformation matrix is following.

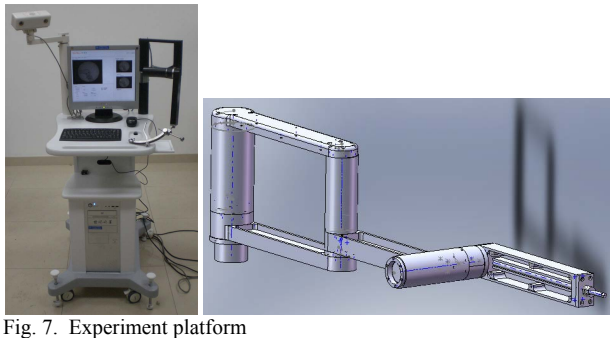

Fig. 7. Experiment platform

$$A_4 = Rot(Z_3,\theta_4)Rot(X_3,\varphi_4)Rot(Y_3,\psi_4)Trans(0,d_4,0)$$

$$= \begin{bmatrix} \cos\theta_4 & -\sin\theta_4 & 0 & 0 \\ \sin\theta_4 & \cos\theta_4 & 0 & 0 \\ 0 & 0 & 1 & 0 \\ 0 & 0 & 0 & 1 \end{bmatrix} \begin{bmatrix} 1 & 0 & 0 & 0 \\ 0 & \cos\varphi_4 & -\sin\varphi_4 & 0 \\ 0 & \sin\varphi_4 & \cos\varphi_4 & 0 \\ 0 & 0 & 0 & 1 \end{bmatrix} \begin{bmatrix} \cos\psi_4 & 0 & \sin\psi_4 & 0 \\ 0 & 1 & 0 & 0 \\ -\sin\psi_4 & 0 & \cos\psi_4 & 0 \\ 0 & 0 & 0 & 1 \end{bmatrix} \begin{bmatrix} 1 & 0 & 0 & 0 \\ 0 & 1 & 0 & d_4 \\ 0 & 0 & 1 & 0 \\ 0 & 0 & 0 & 1 \end{bmatrix}$$

$$= \begin{bmatrix} \cos\theta_4\cos\psi_4 - \sin\theta_4\sin\varphi_4\sin\psi_4 & -\sin\theta_4\cos\varphi_4 & \cos\theta_4\sin\psi_4 + \sin\theta_4\sin\varphi_4\cos\psi_4 & -d_4\sin\theta_4\cos\psi_4 \\ \sin\theta_4\cos\psi_4 + \cos\theta_4\sin\varphi_4\sin\psi_4 & \cos\theta_4\cos\varphi_4 & \sin\theta_4\sin\psi_4 - \cos\theta_4\sin\varphi_4\cos\psi_4 & d_4\cos\theta_4\cos\varphi_4 \\ -\cos\varphi_4\sin\psi_4 & \sin\varphi_4 & \cos\varphi_4\cos\psi_4 & d_4\sin\varphi_4 \\ 0 & 0 & 0 & 1 \end{bmatrix}$$

According to the design method and ideal, 6 DOFS robot is developed finally, as shown in Fig.7.

IV. EXPERIMENTS

Fig.8. Experiment platform

TABLE II
RESULTS OF TRACKING THE INSERTION POINT PLANNED

Serial number	*Instrument's coordinate/mm*			*Real coordinate/mm*			*Error/mm*
	X	Y	Z	X	Y	Z	Distance
1	22.09	50.79	1.22	23.08	51.27	-173.53	1.22
2	1.30	50.96	0.97	1.09	51.67	-179.36	0.97
3	7.43	33.23	2.70	9.89	34.13	-166.06	2.70
4	-12.03	32.84	0.80	-11.65	33.24	-169.15	0.80
5	-4.23	20.23	1.56	-2.99	21.04	-168.75	1.56
6	4.03	1.73	0.79	4.13	2.44	-162.59	0.79
7	-20.72	4.40	2.59	-21.24	3.39	-166.17	2.59
8	4.17	-16.56	2.14	4.70	-15.14	-179.76	2.14

Average of the distance between two points/mm: 1.59 mm

A. System precision experiments

The experiments include precision analysis, simulation and evaluation on the femoral quadrant and tibial Stäublis. Install the dynamic reference base (DRB) made on the two-layer correction board, operation instrument and anatomical limb. Then place the correction board on the c-arm and registration as shown in Fig.8. The real operation instrument is replaced by the probe of Micron Tracker as shown in 3 of Fig.2. And the planning results on x-ray image are shown in Fig.9.

The surgeon can detect the insertion points on femur and tibia with the probe in real-time tracking of Micron Tracker. When the projection of the tip of probe overlaps with the point planned on the fluoroscopy, this point on plastic pointed by the instrument is the insertion point. Currently, the instrument's projection can be considered as the direction of the implantation tunnel. As shown in Table 2, 8 sets of points are collected to validate the precision. The surgeon can compute the coordinates of points in real space when the instrument is matching on the fluoroscopy. Compared to the theoretic point, the average distance of precision is 1.59mm and the maximum is 2.59mm. It can satisfy the clinical requirement.

Finally, the surgeon collects the characteristic of the femoral intercondyle and tibia platform with the probe monitored by video camera. Then he can reconstruct the surface and the virtual ACL model in order to simulate the kinematic performance of knee joint. The system will compute the length and elongation value of ACL. As shown in Fig.10, the blue stripe which is 41.04mm long represents the length, and cyan stripe which is 1.97mm long represents the elongation. The results can satisfy the anatomical isometric characteristics defined in medical field, that is, the elongation is no more than 3mm. [14]

Fig.9. Experiment platform

B. Experiments on the 6 DOFS robot

Some experiments on 10 plastic bones (Synbone, Swiss) and 5 animal bones including the navigation assistance in entry planning of tunnels, the real time tracing of surgical apparatus and the end of robot, the individualized surface reconstruction of knee joint, the virtual simulation of the impingement, and anisometry evaluation of reconstructed ACL were implemented. The accuracy tests give out a resulting positioning error less than 1.6 mm. The experiment

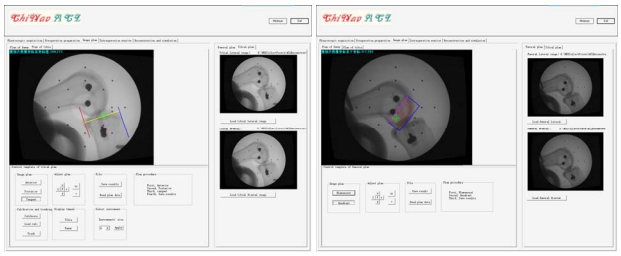

Fig.10. Results planned

platform is implemented as shown in Fig.9.

V. DISCUSSION

The experiments include precision analysis, simulation and evaluation on the femoral quadrant and tibial Stäublis. Install

the dynamic reference base (DRB) made on the two-layer correction board, operation instrument and anatomical limb. Then place the correction board on the c-arm and registration as shown in Fig.8. The real operation instrument is replaced by the probe of Micron Tracker as shown in 3 of Fig.2. And the planning results on x-ray image are shown in Fig.10.

The surgeon can detect the insertion points on femur and tibia with the probe in real-time tracking of Micron Tracker. When the projection of the tip of probe overlaps with the point planned on the fluoroscopy, this point on plastic pointed by the instrument is the insertion point. Currently, the instrument's projection can be considered as the direction of the implantation tunnel. As shown in Table 2, 8 sets of points are collected to validate the precision. The surgeon can compute the coordinates of points in real space when the instrument is matching on the fluoroscopy. Compared to the theoretic point, the average distance of precision is 1.59mm and the maximum is 2.59mm. It can satisfy the clinical requirement.

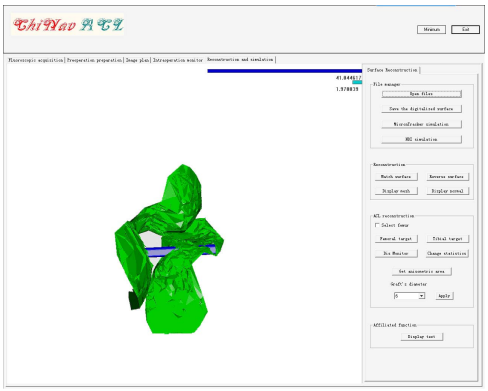

Fig.11. ACL virtual evaluation

Finally, the surgeon collects the characteristic of the femoral intercondyle and tibia platform with the probe monitored by video camera. Then he can reconstruct the surface and the virtual ACL model in order to simulate the kinematic performance of knee joint. The system will compute the length and elongation value of ACL. As shown in Fig.11, the blue stripe which is 41.04mm long represents the length, and cyan stripe which is 1.97mm long represents the elongation. The results can satisfy the anatomical isometric characteristics defined in medical field, that is, the elongation is no more than 3mm.

VI. Conclusions

This work applies computer aided navigation system in ACL reconstruction to plan the operation, detects the collision of graft, and evaluates the isometry. It can improve precision of the insertion points' placement and quality of ACL reconstruction operation. The precision is related with image correction, c-arm registration, video tracking and surface reconstruction closely. Low position error satisfies the requirement of operations, and great clinical application significance has been verified by the experiment. And the function of 6 DOFS can satisfy the requirement of the navigation system.

Acknowledgment

Y. Hu thanks J.C. Wang, Q.W. Bian, Y.G. Xu, as well as Prof. M.Y. Wang and Prof. R.Y. Huang for their support in this study. Furthermore, the authors are indebted to S. Luan and J. Zhao for their assistance in image data acquisition and processing.

References

[1] Klos, T.S., Banks A.Z., Cook F.F.. Computer-assisted anterior cruciate ligament reconstruction. Computer Assisted Orthopedic Surgery (CAOS). Bern: Hogrefe & Huber Publishers, 1999: 184 - 189.

[2] Howe J.G., Johnson R.J., Kaplan M.J., Fleming B., Jarvinen M.. Anterior cruciate ligament reconstruction using quadriceps patellar tendon graft, part I: Long term follow up. Am J Sports Med, 1991, 19: 447 - 457.

[3] Paessler H.H., Hoeher J.: Intraoperative quality control of the placement of bone tunnels for reconstruction of the anterior cruciate ligament. *Unfallchirurg*, 2004, 107: 263 - 272.

[4] Shafizadeh S, Paffrath T, Grote S, Hoeher J., Tiling Th., Bouillon B.. Fluoroscopic-based ACL Navigation. Navigation and MIS in Orthopedic Surgery, Berlin, German: Springer, 2007: 324 - 332.

[5] Kuga M., Yasuda K., Hata N., Dohi T.. Navigation System for ACL Reconstruction Using Registration between Multi-Viewpoint X-ray Images and CT Images. International Cong-ress and Exhibition on Computer Assisted Radiology and Su-rgery, Chicago, USA, 2004, 1268: 498 - 502.

[6] Holmes P.F., James S.L., Larson R.L., Singer K.M., Jones D.C.. Retrospective direct comparison of three intraarticular anterior cruciate ligament reconstructions. Am J Sports Med, 1991, 19: 596 - 600.

[7] Ishibashi Y., Tsuda E., Fukuda A., Tsukada H., Toh S.. Future of double-bundle anterior cruciate ligament (ACL) reconstruction: incorporation of ACL anatomic data into the navigation system. *Orthopedics*, 2006, 29 Suppl: 108 - 112.

[8] Fang J.C., Quan W., Meng X.H.. All-sky autonomous star map identification algorithm based on Delaunay triangulation cutting algorithm. Journal of Beijing University of Aeronautics and Astronautics, 2005, 31(3): 311 - 315.

[9] Jaramaz B., Nikou C., Watterson N.. MRI-based Surgical Navigation System for ACL Reconstruction. *Journal of Biomechanics*, 2006, 39: 573 - 574.

[10] Shafizadeh S., Huber H.J., Grote S., Hoeler J., Paffrath Th., Tiling T.. Principles of Fluoroscopic-Based Navigation in Anterior Cruciate Ligment Reconstruction. *Operative Techniques in Orthopaedics*, 2005, 15: 71 - 75

[11] Wolf A., Digioia A.M., Jaramaz B.. Computer-guided total knee arthroplasty. In: Scuderi GR, Tria AJ, Berger RA. MIS techniques in orthopedics, Springer-Verlag, 2005: 390 - 407.

[12] Fleute M., Lavallée S., Julliard R.. Incorporating a statistically based shape model into a system for computer-assisted anterior cruciate ligament surgery. *Med Image Anal*, 1999, 3: 209 - 222.

[13] Hüfner T., Meller R., Kendoff D., Zeichen J., Zelle B. A., Fu F. H.. The Role of Navigation in Knee Surgery and Evaluation of Three-Dimensional Knee Kinematics. *Operative Techniques in Orthopaedics*, 2005, 15: 64 - 69.

[14] Xu Q.R., Zhu ZH.A.. The effect of the position change of Anterior Cruciate Ligament on the tibia and femur toisometry. Chinese Journal of Trauma, 2005, 21(2): 131 - 133.